

Light scattering by ultracold atoms in an optical lattice

Stefan Rist,¹ Chiara Menotti,² and Giovanna Morigi^{1,3}

¹*Departament de Física, Universitat Autònoma de Barcelona, E-08193 Bellaterra, Spain*

²*CNR-INFM BEC, and Dipartimento di Fisica, Università di Trento, I-38050 Povo, Italy*

³*Theoretische Physik, Universität des Saarlandes, D-66041 Saarbrücken, Germany*

(Received 6 April 2009; published 5 January 2010)

We investigate theoretically light scattering of photons by ultracold atoms in an optical lattice in the linear regime. A full quantum theory for the atom-photon interactions is developed as a function of the atomic state in the lattice along the Mott-insulator–superfluid phase transition, and the photonic-scattering cross section is evaluated as a function of the energy and of the direction of emission. The predictions of this theory are compared with the theoretical results of a recent work on Bragg scattering in time-of-flight measurements [A.M. Rey *et al.*, Phys. Rev. A **72**, 023407 (2005)]. We show that, when performing Bragg spectroscopy with light scattering, the photon recoil gives rise to an additional atomic site-to-site hopping, which can interfere with ordinary tunneling of matter waves and can significantly affect the photonic-scattering cross section.

DOI: [10.1103/PhysRevA.81.013404](https://doi.org/10.1103/PhysRevA.81.013404)

PACS number(s): 37.10.Jk, 42.50.–p, 03.75.Lm, 37.10.Vz

I. INTRODUCTION

Bragg scattering in condensed matter is a powerful method for gaining information over the structural properties of crystalline solids. Usually, one employs thermal neutron beams, whose thermal wavelength is of the order of the interparticle distance inside the crystal. While elastic scattering allows one to measure the reciprocal lattice primitive cell, inelastic scattering gives information about the phonon spectrum and anharmonicities [1]. In atomic systems, Bragg scattering has been applied for demonstrating long-range order in structures of cold ions in traps [2] and neutral atoms in optical lattices [3–7]. Moreover, it has proven to be a precise tool for the measurement of the elementary excitations of trapped Bose-Einstein condensate [8,9] and strongly correlated atoms in optical lattices [10]. The spectra of the scattered photons, moreover, provide information on the details of atom-photon interactions. Studies on optomechanical systems, for instance, showed that the Stokes and anti-Stokes components of the scattered light may exhibit entanglement, which emerges from and is mediated by the interaction with the quantum vibrational modes of the scattering system [11]. Such correlations are endorsed by quantum interference in the processes leading to photon scattering, which is mainly visible in the height of the spectral peaks as a function of the emission angle [12] and can be an important resource for quantum networks [13,14].

In this article, we investigate the optomechanical properties of strongly correlated atoms in optical lattices. These systems present peculiar features, when compared with solid-state crystals. In optical lattices, the bulk periodicity is determined by the light potentials and is hence of the order of half the laser wavelength. One remarkable property is that light both couples to the atomic transition and is diffracted by the crystalline structure which the atoms form [3–5]. This property implies, for instance, that the system may exhibit peculiar self-organization, with the atoms being a diffracting medium for the light which traps them [4,15–17].

In the dispersive regime, when the optical lattice can be considered a conservative potential, various states of ultracold matter can be realized [18], thereby mimicking solid-state

models [19,20], a prominent example of which is the quantum phase transition between a Mott insulator and a superfluid state [21]. Bragg spectroscopy provides an important tool for characterizing the quantum state of the atomic gas [8–10]. The experimental procedure typically uses two laser beams, whose wave-vector difference \mathbf{q} gives, by means of the mechanical effects induced by photon recoil, a momentum and energy transfer $\hbar\mathbf{q}$ and $\hbar\omega$ [8]. The corresponding atomic response is detected by a time-of-flight measurement, consisting of releasing the trap and measuring the momentum distribution by atom detection [8,9]. An alternative procedure makes use of parametric amplification followed by time-of-flight measurement, thereby revealing the energy transfer and the spectrum [22,23]. These procedures may allow one to measure the structure form factor [24–26] and characterize the state of the gas.

Most recently, ultracold atoms were loaded inside of optical resonators, and first measurements of the spectrum of transmission of the light at the cavity output showed novel features, which can be brought back to the collective and coherent interaction of the atoms with the light [17,27–30]. Several theoretical works pointed out that the observation of the photon scattered by ultracold atoms may provide complementary information on the quantum state of the atoms [31–35], which could be nondestructive in some setups [34,36].

We also remark that theoretical studies on fermionic systems in an optical lattice showed that intensity fluctuations of the scattered light may allow one to determine the temperature of the atomic cloud [37]. Optical detection, and in particular the intensity of the Bragg peaks, were proposed as a mean for revealing fractional particle numbers of Fermi gases confined by optical lattices [38]. In this article, we study light scattering by ultracold bosonic atoms in an optical lattice, as in the setup sketched in Fig. 1. We use a full quantum description of the photonic and atomic fields for a range of optical lattice depths which covers the superfluid-to-Mott-insulator transition. By starting from the general Hamiltonian, we carry out the tight-binding and single-band approximations, and we determine the scattering cross section of photons in the linear response regime. Extending previous works [32], we systematically take into account the finite tunneling rate in evaluating the

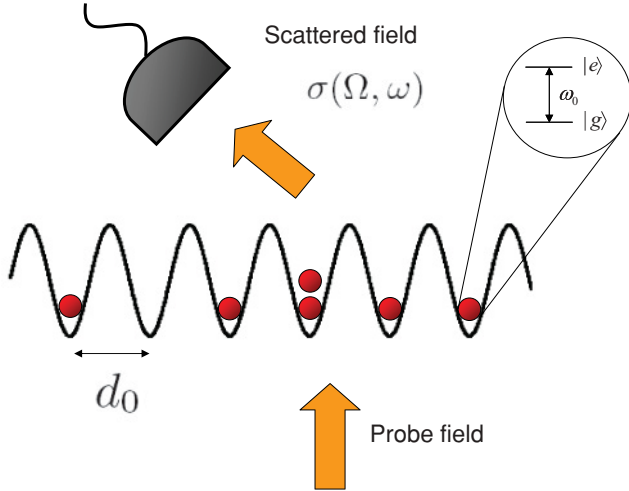


FIG. 1. (Color online) Light scattering by atoms trapped in a one-dimensional optical lattice with lattice constant d_0 . The atoms are probed by a laser beam, with wave vector k_L and frequency ω_L , which couples to the atomic dipole transition at frequency ω_0 with ground state $|g\rangle$ and excited state $|e\rangle$ (see inset). The spectrum of the scattered light is measured at a detector as a function of the angle of emission. In experiments, one can also use a second laser beam, into which the photon is emitted with high probability, hence, implementing stimulated Bragg scattering [8].

scattering cross section for parameters sweeping along the phase-transition Mott insulator to superfluid state. Our study focuses on a small lattice of seven sites and solves numerically the Bose-Hubbard model for this system. In order to get insight into the numerical results, we also develop an analytical theory, which extends the theory presented in [24] by including the hopping induced by photon recoil. The interference between the finite tunneling rate and the photon-induced hopping is visible in the height of the Stokes peaks as a function of the emission angle and can be revealed experimentally.

This article is organized as follows: In Sec. II, we present the theoretical model. In Sec. III, the scattering cross section is evaluated both analytically and by means of numerical simulations. The conclusions are discussed in Sec. IV.

II. THE MODEL

The scattering system we consider is composed by N identical bosonic atoms of mass m in a periodic potential, as shown in Fig. 1. The relevant internal degrees of freedom of the atoms are the electronic ground state $|g\rangle$ and an excited state $|e\rangle$ that form a dipolar transition with dipole moment \mathbf{D} at the optical frequency ω_0 , which couples to a weak laser probe. The Hamiltonian in second quantization reads as $H = H_{\text{at}} + H_{\text{emf}} + H_{\text{int}}$ with [39]

$$H_{\text{at}} = \hbar\omega_0 \int d\mathbf{r} \psi_e^\dagger(\mathbf{r}) \psi_e(\mathbf{r}) + \sum_{j=e,g} H_j + H_{eg}, \quad (1)$$

$$H_{\text{emf}} = \sum_{\lambda} \hbar\omega_{\lambda} a_{\lambda}^{\dagger} a_{\lambda}, \quad (2)$$

where by $\psi_j(\mathbf{r})$ and $\psi_j^\dagger(\mathbf{r})$ we denoted the annihilation and creation operators of an atom in the internal state $j = g, e$

at position \mathbf{r} , and by a_{λ} and a_{λ}^{\dagger} the annihilation and creation operators of a photon in the mode at frequency ω_{λ} , wave vector \mathbf{k}_{λ} , and polarization $\boldsymbol{\epsilon}_{\lambda} \perp \mathbf{k}_{\lambda}$. The atomic field operators obey the bosonic commutation relations $[\psi_j(\mathbf{r}), \psi_{j'}(\mathbf{r}')] = [\psi_j^\dagger(\mathbf{r}), \psi_{j'}^\dagger(\mathbf{r}')] = 0$ and $[\psi_j(\mathbf{r}), \psi_{j'}^\dagger(\mathbf{r}')] = \delta_{jj'} \delta(\mathbf{r} - \mathbf{r}')$. The Hamiltonian term H_g , (H_e) describes the motion of the atoms in the internal state $|g\rangle$ ($|e\rangle$), and H_{eg} gives the collisional interaction between the atoms in states $|g\rangle$ and $|e\rangle$. We will assume that the atoms interact with radiation far-off resonance from the dipolar transition; hence, the occupation of the excited state is small and will be neglected. Therefore, we just need to provide the detailed form of the ground-state term

$$H_g = \int d\mathbf{r} \psi_g^\dagger(\mathbf{r}) \left(-\frac{\hbar^2 \nabla^2}{2m} + V(\mathbf{r}) \right) \psi_g(\mathbf{r}) + \frac{u_{gg}}{2} \int d\mathbf{r} \psi_g^\dagger(\mathbf{r}) \psi_g^\dagger(\mathbf{r}) \psi_g(\mathbf{r}) \psi_g(\mathbf{r}), \quad (3)$$

where u_{gg} is the strength of the contact interaction. The potential $V(\mathbf{r})$ is assumed to be periodic along the x direction and reads as

$$V(\mathbf{r}) = V_0 \sin^2 \left(\frac{\pi x}{d_0} \right) + \frac{1}{2} m \omega_r (y^2 + z^2), \quad (4)$$

where V_0 is the lattice depth, d_0 is the lattice constant, and ω_r is the frequency of the harmonic trap which tightly confines the transverse motion.

Finally, the interaction term between atoms and light reads (in the length gauge) as

$$H_{\text{int}} = \sum_{\lambda} \hbar C_{\lambda} \int d\mathbf{r} \psi_e^\dagger(\mathbf{r}) \psi_g(\mathbf{r}) a_{\lambda} e^{i\mathbf{k}_{\lambda} \cdot \mathbf{r}} + \text{H.c.}, \quad (5)$$

where

$$C_{\lambda} = \sqrt{\frac{\omega_{\lambda}}{2\hbar\epsilon_0\mathcal{V}}} (\mathbf{D} \cdot \boldsymbol{\epsilon}_{\lambda}) \quad (6)$$

is the coupling strength, with ϵ_0 the vacuum electric permittivity and \mathcal{V} the quantization volume.

A. Linear response

At room temperature and equilibrium, the atoms are in the electronic ground state and the state of the optical modes of the electromagnetic field can be approximated with the vacuum $|0\rangle$. We now assume that a laser, at frequency ω_L and wave vector k_L , couples to the atomic dipole transition. The laser field is described by a coherent state of the corresponding electromagnetic field mode with amplitude α_L , such that the mean number of photons is given by $|\alpha_L|^2$. In the regime in which the atom-laser coupling is sufficiently weak, corresponding to the condition $|C_L \alpha_L| \ll |\omega_0 - \omega_L|$, we eliminate the excited state from the equations of motion of the ground state in second-order perturbation theory in the small parameter $|C_L \alpha_L|/|\omega_0 - \omega_L|$. The dynamics of the atoms in the electronic ground state $|g\rangle$ is now described by the effective Hamiltonian

$$H_{\text{eff}} = H_g + H_{\text{emf}} + H'_{\text{int}}, \quad (7)$$

where the interaction term takes the form

$$\begin{aligned} H'_{\text{int}} &= \hbar \sum_{\lambda, \lambda'} \frac{C_{\lambda}^* C_{\lambda'}}{\omega_{\lambda'} - \omega_0} a_{\lambda}^{\dagger} a_{\lambda'} \int d\mathbf{r} e^{i\mathbf{q}\cdot\mathbf{r}} \psi_g^{\dagger}(\mathbf{r}) \psi_g(\mathbf{r}) \\ &= \hbar \sum_{\lambda, \lambda'} \frac{C_{\lambda}^* C_{\lambda'}}{\omega_{\lambda'} - \omega_0} a_{\lambda}^{\dagger} a_{\lambda'} \mathcal{N}_{\mathbf{q}} \end{aligned} \quad (8)$$

and describes the absorption of a photon in the mode λ' and wave vector $\mathbf{k}_{\lambda'}$ and the emission into the mode λ and wave vector \mathbf{k}_{λ} , weighted by the Fourier transform of the density $\mathcal{N}_{\mathbf{q}} = \int d\mathbf{r} e^{i\mathbf{q}\cdot\mathbf{r}} \psi_g^{\dagger}(\mathbf{r}) \psi_g(\mathbf{r})$, with

$$\mathbf{q} = \mathbf{k}_{\lambda'} - \mathbf{k}_{\lambda}. \quad (9)$$

In the following, we will assume that the interaction between photons and atoms is essentially Hamiltonian and, hence, fully determined by the Schrödinger equation governed by Eq. (7). This is valid in the regime which we consider in this article, namely, when the detuning of the light $|\omega_0 - \omega_L| \gg \gamma$, with γ the linewidth of the excited state.

In this work, we study Bragg scattering of laser photons by atoms in the one-dimensional periodic array given by potential (4). We will hence evaluate the differential scattering cross section for coherent scattering. Assuming that $|\alpha_L| \ll 1$, so that the atoms absorb at most one photon from the laser at a time, the differential scattering cross section is found from the rate of scattering one laser photon into the mode λ . In particular, the scattering rate reads as

$$\begin{aligned} \Gamma_{\lambda_L \rightarrow \lambda} &= \frac{2\pi}{\hbar^2} \sum_f |(1_{\lambda}, f| H'_{\text{int}} |1_{\lambda_L}, i)|^2 \\ &\times \delta^{(T)}(\omega_L - \omega_{\lambda} + (E_i - E_f)/\hbar), \end{aligned} \quad (10)$$

where we denoted by $|1_{\lambda}\rangle = a_{\lambda}^{\dagger}|0\rangle$ the state of the electromagnetic field with one photon in mode λ and by $|i\rangle$ and $|f\rangle$ the states of the atoms before and after the scattering, respectively, which are eigenstates of Hamiltonian H_g at energies E_i and E_f . The function

$$\delta^{(T)}(\omega) = \frac{\sin(\omega T/2)}{\pi \omega} \quad (11)$$

is the diffraction function, giving energy conservation for infinite interaction times, $\lim_{T \rightarrow \infty} \delta^{(T)}(\omega) = \delta(\omega)$ [40].

Equation (10) shows clearly that the scattering rate depends on the state of the atoms before and after the scattering event. In the following, we derive the atom-light interaction Hamiltonian in the tight-binding approximation and conclude this section by introducing the many-body atomic states which are relevant for the scattering process considered here.

B. Tight-binding regime

We assume that the atomic wave functions are well localized at the lattice minima, such that the tight-binding approximation can be applied. Furthermore, at ultralow temperature and not too strong interactions, the atomic gas is in the lowest band of the periodic potential and in the ground state of the radial oscillator, so that the atomic-field operator can be decomposed as

$$\psi_g(\mathbf{r}) = \phi_0(\rho) \sum_l w_l(x) b_l, \quad (12)$$

where $w_l(x) = w(x - ld_0)$ is the Wannier function centered at position ld_0 , with the sum going over all lattice sites, and $\phi_0(\rho) = \exp(-\rho^2/2\xi_r^2)/(\xi_r \sqrt{\pi})$ is the ground state of the radial oscillator ($\rho = \sqrt{y^2 + z^2}$) with $\xi_r = \sqrt{\hbar/m\omega_r}$. The operators b_l annihilate an atom at site l and fulfill the standard bosonic commutation relations $[b_l, b_{l'}^{\dagger}] = \delta_{l,l'}$. Using this decomposition in Eq. (3), allowing only nearest-neighbor hopping and restricting to on-site atom-atom interactions, we obtain the Bose-Hubbard Hamiltonian [19]

$$H'_g = -J \sum_l b_l^{\dagger} (b_{l-1} + b_{l+1}) + \frac{U}{2} \sum_l n_l (n_l - 1) - \mu \sum_l n_l, \quad (13)$$

where $n_l = b_l^{\dagger} b_l$ is the atomic number operator at site l and μ is the chemical potential. The coefficients for the hopping term and the on-site interaction strength read as

$$J = - \int dx w_l(x) \left(-\frac{\hbar^2 \nabla^2}{2m} + V(x) \right) w_{l+1}(x), \quad (14)$$

$$U = u_{gs} \frac{m\omega_r}{4\pi\hbar} \int dx w_l(x)^4, \quad (15)$$

with the Wannier functions chosen to be real. Note that frozen transverse dynamics, as assumed in Eq. (12), is here ensured by taking $J, U \langle n \rangle \ll \hbar\omega_r$, where $\langle n \rangle$ is the mean site occupation. Within this decomposition, the term describing atom-light scattering takes the form

$$H'_{\text{int}} = \sum_{\lambda, \lambda'} \frac{\hbar C_{\lambda}^* C_{\lambda'}}{\omega_{\lambda'} - \omega_0} a_{\lambda}^{\dagger} a_{\lambda'} \mathcal{T}(\mathbf{q}). \quad (16)$$

Here,

$$\mathcal{T}(\mathbf{q}) = \sum_l e^{i\mathbf{q}\cdot l d_0} [J_0(\mathbf{q}) n_l + J_1(\mathbf{q}) (b_l^{\dagger} b_{l+1} + b_{l+1}^{\dagger} b_l)] \quad (17)$$

consists of a photon-dependent energy shift, weighted by the coefficient

$$J_0(\mathbf{q}) = e^{-\frac{1}{4}(q_y^2 + q_z^2)\xi_r^2} \int dx e^{i\mathbf{q}\cdot x} w_0(x)^2, \quad (18)$$

and a hopping term with coefficient

$$J_1(\mathbf{q}) = e^{-\frac{1}{4}(q_y^2 + q_z^2)\xi_r^2} \int dx w_0(x) e^{i\mathbf{q}\cdot x} w_0(x - d_0), \quad (19)$$

which describes light-assisted tunneling due to the mechanical effects of photon scattering. This latter term has been neglected in previous theoretical treatments [24,32,33]. Its effect has been investigated in Ref. [31,41] for light scattering by ultracold atoms in a double-well potential, showing that the mechanical effect of light can interfere with ordinary tunneling between the wells, generating observable effects in the first-order coherence properties of the scattered light. We hence expect that it will give rise to observable effects in the Bragg signal by ultracold atoms in optical lattices.

In the following, we introduce the many-body states, eigenstates of H'_g , which are relevant for the scattering process when the system is in the Mott insulator and in the superfluid regime. In this treatment, we use the same notations as in Ref. [42] and refer the reader to this work for more details, like, for example, the careful comparison between the

Bogoliubov approximation and the exact solution for small one-dimensional systems.

I. Mott-insulator state

For vanishing hopping, the ground state of Hamiltonian (13) is the Mott-insulator state with all lattice sites equally occupied with (integer) filling factor $g = N/M$,

$$|\psi_0^{(0)}\rangle = \prod_{l=1}^M \frac{(b_l^\dagger)^g}{\sqrt{g!}} |0\rangle_{\text{at}} = |g, g, \dots, g, g\rangle, \quad (20)$$

where $|0\rangle_{\text{at}}$ denotes the vacuum. The corresponding ground state energy for $J = 0$ is easily found and reads as $E_0^0 = MUg(g-1)/2 - Mg\mu$. The lowest lying excitations take the form

$$|\psi_{n,m}^{(0)}\rangle = \frac{b_n^\dagger b_m}{\sqrt{g(g+1)}} |\psi_0^{(0)}\rangle, \quad (21)$$

where one particle and one hole are created at site n and m , respectively, with energy $E_1^0 = E_0^0 + U$. These states form a degenerate subspace of dimension $M(M-1)$. This degeneracy is lifted for finite values of the hopping J .

The corrections due to a nonvanishing but small value of tunneling are evaluated using perturbation theory. Including the first-order correction, the ground state now reads as

$$|\psi_0^{(1)}\rangle = \left[1 - \frac{J^2}{U^2} Mg(g+1)\right] |\psi_0^{(0)}\rangle + \frac{J}{U} \sqrt{2Mg(g+1)} |S\rangle, \quad (22)$$

where $|S\rangle = \frac{1}{\sqrt{2M}} \sum_n (|\psi_{n,n+1}^{(0)}\rangle + |\psi_{n,n-1}^{(0)}\rangle)$ is the normalized state of adjacent particle-hole excitations, while the term at second order in J warrants normalization of state (22). The corresponding energy is $E_0 = E_0^0 + O(J^2)$. The lowest lying excitations are determined using degenerate perturbation theory within the subspace of single particle-hole excitations,

$$|\psi_{[i]}^{(0)}\rangle = \sum_{n,m} c_{n,m}^{[i]} |\psi_{n,m}^{(0)}\rangle, \quad (23)$$

where the coefficients $c_{n,m}^{[i]}$ fulfill the normalization condition and satisfy the equations

$$(g+1)(c_{n+1,m}^{[i]} + c_{n-1,m}^{[i]}) + g(c_{n,m+1}^{[i]} + c_{n,m-1}^{[i]}) = A_i c_{n,m}^{[i]}, \quad (24)$$

with periodic boundary conditions

$$c_{n+M,m}^{[i]} = c_{n,m+M}^{[i]} = c_{n,m}^{[i]}, \quad (25)$$

$$c_{n,n}^{[i]} = 0. \quad (26)$$

Term A_i in Eq. (24) is the first-order correction to the corresponding energy, $E_i = E_0 + U - JA_i + O(J^2)$.

An analytic solution of Eq. (24) can be derived in the limit of large filling $g \gg 1$ [24,42]. This limit introduces a symmetry between particle and hole excitations that simplifies the analytical treatment but imposes a selection rule, which is strictly correct only when $g \rightarrow \infty$. The coefficients, evaluated

in this limit, read as

$$c_{n,m}^{[r,s]} = \frac{\sqrt{2}}{M} \times \begin{cases} \sin[\alpha r |n-m|] e^{i\alpha s(n+m)} & \text{for } r+s \text{ odd,} \\ \sin[\alpha r(n-m)] e^{i\alpha s(n+m)} & \text{for } r+s \text{ even,} \end{cases} \quad (27)$$

with $\alpha = \frac{\pi}{M}$, $s = 0, 1, \dots, M-1$ and $r = 1, 2, \dots, M-1$. Correspondingly, the lowest lying excitations and their energy read (at first order in J and for $g \gg 1$) as

$$|\psi_{[r,s]}^{(1)}\rangle = \begin{cases} \frac{1}{\mathcal{N}_r} \left[\sum_{n,m} (c_{n,m}^{[r,0]} |\psi_{n,m}\rangle) - \frac{J}{U} \sqrt{8g(g+1)} \sin \alpha r |\psi_0^{(0)}\rangle \right] & \text{for } s=0 \text{ and } r \text{ odd,} \\ \sum_{n,m} c_{n,m}^{[r,s]} |\psi_{n,m}\rangle & \text{otherwise,} \end{cases} \quad (28a)$$

$$E_{r,s} = E_0^0 + U - 2J(2g+1) \cos \alpha r \cos \alpha s + O(J^2), \quad (28b)$$

where \mathcal{N}_r is a normalization factor. Note that states $|\psi_{[r,s]}^{(1)}\rangle$ contain a correction proportional to the ground state $|\psi_0^{(0)}\rangle$. This correction is found from nondegenerate perturbation theory and warrants the orthonormality of the new basis $\{|\psi_0^{(1)}\rangle, |\psi_{[r,s]}^{(1)}\rangle\}$.

2. Superfluid state

In the weakly interacting superfluid regime, quantum fluctuations in the number of atoms per site are described by the decomposition

$$b_l = z_l + \beta_l, \quad (29)$$

where z_l is a complex number describing the order parameter and β_l is the fluctuations operator obeying the bosonic commutation rules. The order parameter z_l is found by minimizing Hamiltonian (13) at zeroth order in the expansion in β_l and β_l^\dagger . It obeys the discrete nonlinear Schrödinger equation

$$\mu z_l = - \sum_{(k,m)} J_k z_m \delta_{k,l} + U |z_l|^2 z_l, \quad (30)$$

where $|z_l|^2$ corresponds to the condensate fraction. For a translationally invariant lattice and in the limit of weak interactions, as considered here, it is given by $|z_l|^2 = g$, and Eq. (30) reduces to

$$\mu = -2J + Ug. \quad (31)$$

Using Eqs. (29) and (30) in Hamiltonian (13), keeping only terms up to second order in the operators β_l, β_l^\dagger , one finds $H'_g = H_0 + H_2$ with

$$H_2 = \sum_{l,m} \mathcal{L}_{l,m} \beta_l^\dagger \beta_m + \mathcal{M}_{l,m} \beta_l^\dagger \beta_m^\dagger + \text{H.c.}, \quad (32)$$

where the coefficients read as

$$\mathcal{L}_{l,m} = -J \sum_{(n,k)} \delta_{n,l} \delta_{m,k} / 2 + \delta_{l,m} (2Ug - \mu) / 2, \\ \mathcal{M}_{l,m} = Ug \delta_{l,m} / 2.$$

Term H_2 describes the dynamics of the noncondensed fraction at leading order. It can be written in the diagonal form

$$H_2 = \sum_{p \neq 0} \hbar \Omega_p (\alpha_p^\dagger \alpha_p + \frac{1}{2}) - \sum_l \mathcal{L}_{ll}, \quad (33)$$

where operators α_p and α_p^\dagger are, respectively, the bosonic annihilation and creation operators of the Bogoliubov excitation with quasimomentum $p = n2\pi/Md_0$, with $n = -M, M-1, \dots, M-1$, and the frequency Ω_p is given by

$$\hbar^2 \Omega_p^2 = \epsilon_p^2 + 2Ug\epsilon_p, \quad (34)$$

with

$$\epsilon_p = 4J \sin^2 \left(\frac{d_0 p}{2} \right). \quad (35)$$

Operators $\alpha_p, \alpha_p^\dagger$ satisfy the commutation relations $[\alpha_p, \alpha_{p'}^\dagger] = \delta_{p,p'}$ and are related to β_l by the Bogoliubov transformation

$$\beta_l = \frac{1}{\sqrt{M}} \sum_{p \neq 0} e^{ipld_0} u_p \alpha_p - e^{-ipld_0} v_p \alpha_p^\dagger. \quad (36)$$

The Bogoliubov amplitudes u_p, v_p satisfy the equation $|u_p|^2 - |v_p|^2 = 1$, as a consequence of the commutation relations, and depend only on the modulus of the quasimomentum, $u_p = u_{-p}, v_p = v_{-p}$. They are solutions of the Bogoliubov-de Gennes equations, which in our case read as

$$\begin{pmatrix} J\epsilon_p + Ug & -Ug \\ Ug & -J\epsilon_p - Ug \end{pmatrix} \begin{pmatrix} u_p \\ v_p \end{pmatrix} = \hbar \Omega_p \begin{pmatrix} u_p \\ v_p \end{pmatrix}. \quad (37)$$

In particular,

$$u_p^2 = \frac{\epsilon_p + Ug + \hbar \Omega_p}{2\hbar \Omega_p}, \quad (38a)$$

$$v_p^2 = \frac{\epsilon_p + Ug - \hbar \Omega_p}{2\hbar \Omega_p}, \quad (38b)$$

$$u_p v_p = \frac{Ug}{2\hbar \Omega_p}. \quad (38c)$$

We note that ϵ_p is the energy of a noninteracting particle in the lattice. By replacing it with the free-space energy $\epsilon_p \rightarrow p^2/2m$, we recover in Eq. (34) the dispersion relation for a weakly interacting dilute Bose gas in free space [43]. Contrary to the case of the uniform one-dimensional system, where Bogoliubov theory is not applicable, for a finite system, it provides a well-defined and small depletion for $U/J \ll 1$ and large filling. The corresponding spectrum of the differential scattering cross section will be compared here with the numerical results obtained for a finite Bose-Hubbard model composed of seven atoms.

In the following, we will denote by $|0\rangle_{\text{SF}}$ the superfluid state, where all atoms are in the condensate, and by $|p\rangle_{\text{SF}} = \alpha_p^\dagger |0\rangle_{\text{SF}}$ the state with one Bogoliubov excitation at quasimomentum p . In particular, we will consider scattering processes, such that the state of the atoms will include at most one Bogoliubov excitation. To this aim, it is convenient to rewrite operator $\mathcal{T}(\mathbf{q})$ in Eq. (17) using the decomposition of operator b_l in

Eq. (29),

$$\mathcal{T}_{\text{SF}}(\mathbf{q}) = \mathcal{T}_{\text{SF}}^{(0)}(\mathbf{q}) + \mathcal{T}_{\text{SF}}^{(1)}(\mathbf{q}) + \mathcal{T}_{\text{SF}}^{(2)}(\mathbf{q}), \quad (39)$$

The first term on the right-hand side of the equation describes radiation coupling with the condensate and reads as

$$\mathcal{T}_{\text{SF}}^{(0)}(\mathbf{q}) = g (J_0(\mathbf{q}) + 2J_1(\mathbf{q})) \sum_l e^{iq_x l d_0}, \quad (40)$$

while the other terms give radiation coupling with the Bogoliubov excitations and take the form

$$\begin{aligned} \mathcal{T}_{\text{SF}}^{(1)}(\mathbf{q}) = \sqrt{g} \sum_l e^{iq_x l d_0} [J_0(\mathbf{q})(\beta_l + \beta_l^\dagger) \\ + J_1(\mathbf{q})(\beta_l^\dagger + \beta_{l+1} + \beta_{l+1}^\dagger + \beta_l)], \end{aligned} \quad (41)$$

$$\mathcal{T}_{\text{SF}}^{(2)}(\mathbf{q}) = \sum_l e^{iq_x l d_0} [J_0(\mathbf{q})\beta_l^\dagger \beta_l + J_1(\mathbf{q})(\beta_l^\dagger \beta_{l+1} + \beta_{l+1}^\dagger \beta_l)], \quad (42)$$

where the superscript gives the order in the Bogoliubov expansion.

III. LIGHT SCATTERING

Light scattering by a one-dimensional optical lattice of ultracold atoms is studied in the setup sketched in Fig. 1. A laser plane wave at wave vector \mathbf{k}_L , at frequency $\omega_L = c|\mathbf{k}_L|$, and in a coherent state with amplitude α_L drives the atoms. We evaluate the scattered light as a function of the angle of emission, determined by the wave vector \mathbf{k} of the mode into which the photon is emitted, and of the frequency of the emitted photon.

The scattering process is evaluated assuming that the laser very weakly excites the atom, so that the atom-photon interaction is described at lowest order by Hamiltonian (8). Furthermore, the condition $|\alpha_L| \ll 1$ means that the atomic sample is driven by at most one photon. A scattering process will then occur with probability $|\alpha_L|^2$ and will consist of the absorption of one incident photon in the mode of the laser, represented by the state $|1_L\rangle$, and the emission of a photon in one of the modes of the electromagnetic field at wave vector \mathbf{k} and polarization $\epsilon_{\mathbf{k}} \perp \mathbf{k}$, represented by the state $|1_{\mathbf{k}, \epsilon}\rangle$. The corresponding differential scattering cross section for the photon scattered at frequency ω in direction \mathbf{n} in the solid angle Ω is proportional to the scattering rate (10) and takes the form [40,44]

$$\begin{aligned} \sigma(\Omega, \omega) = \frac{\mathcal{V}^2 \omega_L^2}{(2\pi)^2 \hbar^2 c^4} \sum_f \sum_{\epsilon_{\mathbf{k}} \perp \mathbf{n}} | \langle f, 1_{\mathbf{k}, \epsilon} | H'_{\text{int}} | i, 1_L \rangle |^2 \\ \times \delta^{(T)}(\omega_L + \omega_i - \omega - \omega_f), \end{aligned} \quad (43)$$

where $\mathbf{k} = \mathbf{n}\mathbf{k}$ and $|i\rangle, |f\rangle$ are the initial and final atomic states, eigenstates of Hamiltonian (13) at the eigenfrequencies ω_i and ω_f , respectively. Using Eq. (8) in Eq. (43), one can easily verify that the differential scattering cross section is proportional to the dynamic structure factor [24].

We evaluate the scattering cross section assuming that the atoms are initially in the ground state either of the Mott insulator or of the superfluid phase, and that the atoms are scattered into a final state belonging to the lowest lying atomic

excitations. Using the form of operator H'_{int} in Eq. (16), Eq. (43) can be written as

$$\sigma(\Omega, \omega) = \sigma^{(0)}(\Omega, \omega) + \sigma^{(1)}(\Omega, \omega), \quad (44)$$

where

$$\sigma^{(0)} = \mathcal{A}(\Omega) |\langle i | \mathcal{T}(\mathbf{q}) | i \rangle|^2 \delta^{(T)}(\omega_L - \omega) \quad (45)$$

gives the elastic component of the scattered light, while

$$\sigma^{(1)} = \mathcal{A}(\Omega) \sum_f |\langle f, \mathbf{1}_k | \mathcal{T}(\mathbf{q}) | i, \mathbf{1}_L \rangle|^2 \delta^{(T)}(\omega_L - \omega - \delta\omega_f) \quad (46)$$

describes the scattering events in which one mechanical excitation at frequency $\delta\omega_f$ is absorbed from the photon by the atomic lattice (Stokes component) and corresponds to the one-phonon terms in neutron scattering [1]. The corresponding phonon emission processes, giving the anti-Stokes component, are here absent as initially the atoms are in the ground state. Moreover, higher order terms, corresponding to higher order phonon terms in neutron scattering, are here neglected as we assume that at most one mechanical excitation is exchanged between lattice and photons.

The operator $\mathcal{T}(\mathbf{q})$ in the above equations is given in Eq. (17), while the coefficient $\mathcal{A}(\Omega)$ depends on the angle of emission and takes the form

$$\begin{aligned} \mathcal{A}(\Omega) &= \frac{\mathcal{V}^2 \omega_L^2}{(2\pi)^2 \epsilon_0^2 \hbar^2 c^4} \sum_{\epsilon_{\mathbf{k}\perp\mathbf{n}}} \frac{\hbar^2 |C_L C_{\mathbf{k}}|^2}{|\omega_L - \omega_0|^2} \\ &= \frac{\gamma}{c} \frac{\Omega_0^2}{\Delta^2} \left[\frac{3}{8\pi} \left(1 - \frac{|\mathbf{D} \cdot \mathbf{n}|^2}{|\mathbf{D}|^2} \right) \right], \end{aligned} \quad (47)$$

where γ is the linewidth of the dipole transition, $\Delta = \omega_L - \omega_0$ is the detuning of the laser from the atomic transition, and $\Omega_0 = \sqrt{\omega_L / 2\hbar\epsilon_0} \mathbf{D} \cdot \boldsymbol{\epsilon}_L$.

A. Scattering cross section as a function of the atomic state

We now give an analytic expression for the scattering cross section in Eq. (44) for the initial and final states determined in Secs. II B 1 and II B 2.

1. Mott insulator

For the Mott-insulator phase, the initial state is $|i\rangle = |\psi_0^{(1)}\rangle$ given in Eq. (22). Using Eq. (16), we find

$$\begin{aligned} \sigma_{\text{MI}}^{(0)}(\Omega, \omega) &= \mathcal{A}(\Omega) N^2 \delta(\omega_L - \omega) \delta_{q_x, G}^{(M)} \\ &\times \left(|J_0(\mathbf{q})|^2 + 4\sqrt{g(g+1)} \frac{J}{U} \text{Re}\{J_0^*(\mathbf{q}) J_1(\mathbf{q})\} \right), \end{aligned} \quad (48)$$

where G are the vectors of the (one-dimensional) reciprocal lattice and

$$\delta_{q, G}^{(M)} \equiv \frac{1}{M^2} \frac{\sin^2(Md_0q/2)}{\sin^2(d_0q/2)} \quad (49)$$

gives conservation of the Bloch momentum in a finite lattice with M sites, such that $\delta_{q, G}^{(M)} \rightarrow \delta_{q, G}$ (Kronecker delta) as $M \rightarrow \infty$. In Eq. (48), we omitted terms at third and higher order in J and $J_1(\mathbf{q})$. This approximation will be applied to

the rest of this section, assuming that these higher order terms can be neglected.

The presence of $\delta_{q_x, G}^{(M)}$ in Eq. (48) expresses the von-Laue condition for Bragg scattering. At zero order in the hopping term, Eq. (48) gives the response of a crystal of particles oscillating around their equilibrium position. In fact, using a Gaussian ansatz for the wave functions, one can estimate $|J_0(\mathbf{q})|^2 \simeq e^{-2W}$, with $W = [q_x^2 \xi_x^2 + (q_y^2 + q_z^2) \xi_r^2]/8$, where ξ_x and ξ_r are the widths of the atomic wave functions in the axial and radial direction, showing explicitly that this term is analogous to the Debye-Waller factor [1,45]. The term proportional to J is instead a novel feature with respect to traditional condensed-matter systems that arises from light-induced tunneling.

The Stokes component for the Mott insulator is evaluated taking the final states $|f\rangle = |\psi_{[r,s]}^{(1)}\rangle$ given in Eq. (28) and reads as

$$\begin{aligned} \sigma_{\text{MI}}^{(1)}(\Omega, \omega) &= \mathcal{A}(\Omega) \sum_{r,s} \sin^2\left(\frac{\pi r}{M}\right) |\mathcal{B}_{r,s}|^2 \\ &\times \delta(\omega_L - \omega - \omega_{r,s}) \delta_{q(s), G}^{(M)}, \end{aligned} \quad (50)$$

with $\omega_{r,s} = (E_{r,s} - E_0)/\hbar$, and where we have introduced

$$q(s) = q_x - \frac{2\pi}{Md_0} s. \quad (51)$$

The coefficient in Eq. (50) takes the form

$$\begin{aligned} \mathcal{B}_{r,s} &= \sqrt{8g(g+1)} \times \begin{cases} J_1(\mathbf{q}) & \text{for } r+s \text{ odd,} \\ 2 \frac{J}{U} J_0(\mathbf{q}) \sin\left(\frac{\pi}{M} s\right) & \text{for } r+s \text{ even,} \end{cases} \\ & \quad (52) \end{aligned}$$

showing that the transition to the excited states with $r+s$ odd is due to photon recoil and is hence a light-induced hopping process. Note that condition $q(s) = G$ shows that the quantum number s , and more specifically $2\pi s/L$, with $L = Md_0$ the length of the lattice, plays the role of the quasimomentum of the states $|\psi_{r,s}^{(1)}\rangle$. We remark that Eq. (53), for $r+s$ even, agrees with the result evaluated in [24] [see Eq. (9) of that paper for comparison]. The result we find for $r+s$ odd, on the contrary, is discarded in the treatment of [24], as there the authors neglected light-induced hopping terms. In the Mott-insulator regime, these terms are usually very small with respect to the other contributions. They give rise to a significant contribution when interfering with ordinary tunneling. This latter type of contributions is ruled out in the analytical model by the selection rule introduced by the assumption $g \gg 1$, but it is visible in the numerical results, as it will be shown in Sec. III.

2. Superfluid

When evaluating the differential scattering cross section in the superfluid phase, we assume all atoms to be initially prepared in the Bose-Einstein condensate. In addition, for the analytical calculation, we consider the limit $U \rightarrow 0$. In this limit, we can neglect the quantum depletion of the condensate due to the interactions and take the initial state $|i\rangle = |0\rangle_{\text{SF}}$ according to our notation. The zero-phonon term takes now

the form

$$\sigma_{\text{SF}}^{(0)}(\Omega, \omega) = \mathcal{A}(\Omega)\delta(\omega_L - \omega)\delta_{q_x, G}^{(M)} N^2 \left(|J_0(\mathbf{q}) + 2J_1(\mathbf{q})|^2 + 2 \sum_{p \neq 0} \frac{|v_p|^2}{N} \text{Re}\{[J_0(\mathbf{q}) + 2J_1(\mathbf{q})]^* [J_0(\mathbf{q}) + 2J_1(\mathbf{q}) \cos(pd_0)]\} \right), \quad (53)$$

showing that the light-induced tunneling effects enter already at first order in this expression. As in the Mott-insulator case, the analogous of the Debye-Waller factor can be here identified in the term $|J_0(\mathbf{q})|^2$. In this case, though, tunneling effects become more important, modifying significantly the signal as we will show. The first-phonon term reads as

$$\sigma_{\text{SF}}^{(1)}(\Omega, \omega) = \mathcal{A}(\Omega) N \sum_{p \neq 0} \delta(\omega_L - \omega - \Omega_p) \frac{\epsilon_p}{\hbar \Omega_p} \times |(J_0(\mathbf{q}) + J_1(\mathbf{q})(1 + e^{-ipd_0}))|^2 \delta_{q_x - p, G}^{(M)}, \quad (54)$$

and describes the creation of Bogoliubov excitations with quasimomentum $\hbar p$ by photon scattering, such that the relation $p = q_x - G$ holds.

B. Numerical results

In this section, we report the numerical results for the differential scattering cross section obtained when the atoms are in the Mott insulator or in the superfluid state. The numerical results are obtained for a lattice of $M = 7$ sites and a fixed particle number of $N = M$. The coefficient entering the Bose-Hubbard Hamiltonian in Eq. (13) and the operator $\mathcal{T}(\mathbf{q})$ in Eq. (17) are calculated by using the Wannier functions relative to a given lattice depth V_0 of optical potential (4). The Hamiltonian (13) is diagonalized exactly, and the corresponding states are used for determining the differential scattering cross section in Eq. (43). The numerical results are also compared with the analytical predictions of the scattering cross sections reported in the previous section. Although the latter are valid for very large lattices and for large mean-site occupation $g \gg 1$, we find reasonable agreement when comparing these predictions with those for a small lattice of seven sites and single occupancy (see also [24]).

Figures 2(a) and 2(c) display the one-phonon contribution to the differential scattering cross section, $\sigma^{(1)}(\Omega, \omega)$, as a function of the frequency ω and for different scattering angles when the atoms are in the Mott-insulator state. The numerical results are compared with the analytical model (dashed line) and with the model used in the numerical simulations in [24], in which light-induced hopping terms are not considered.

We first discuss the numerical results which most closely approach the exact solution. The appearance of multiple peaks corresponds to the excitations of the atoms in the Mott insulator due to the photon recoil. The number of peaks for the numerical result is $M - 1$, which correspond in this case to 6. They can be individually resolved, as the system considered here is finite, and the width of each individual peak is limited by the detection time T (or the spectral resolution $1/T$) [46]. The analytical results are found using the model described

in Sec. II, which assumes a large on-site occupation. They are characterized by the same peak number, although only half of them is visible in the figure. In fact, the intensity of the peaks arising from the coupling of the ground state to the corresponding excitation via light-induced hopping [corresponding to the terms in Eq. (52) with $r + s$ odd] are very small compared with the other ones (corresponding to the terms with $r + s$ even) and are therefore not visible (note that, due to the assumption of large on-site occupation, interference between ordinary tunneling and light-induced hopping is suppressed). The central positions of the visible peaks present a systematic shift with respect to the ones found numerically. This systematic shift originates from the assumption $g \gg 1$ and has been observed in [24]. Nevertheless, the analytical solution still provides some insight into the numerical results. In Eq. (28), using Eq. (51), we find that the peaks are centered around the energy $E' = U$ with a spreading about this mean value of width $4J(2g + 1) \cos(\frac{q_x d_0}{2})$. Such spreading decreases as $q_x d_0$ approaches π [compare Figs. 2(a) and 2(c)]. In particular, for $q_x d_0 = \pi$, the width of the distribution of the Stokes excitations vanishes and the spectrum reduces to a single peak, corresponding to the on-site energy U .

The results for the superfluid regime are reported in Figs. 2(b) and 2(d). Here, the analytical solution predicts that in the limit $g \gg 1$, the total momentum of photon and lattice is conserved in a scattering event. Such property implies that the Bogoliubov mode matching the momentum-conservation condition is excited, and therefore, one expects a single peak in the spectrum. For $N = 7$ atoms and $g = 1$, the numerical results for $U/J \approx 1$ give a single peak at $q_x d_0 = 2\pi/7$, while at $q_x d_0 = 6\pi/7$, multiple peaks are found. In this case, instead of a collective density fluctuation with a well-defined momentum p , one observes particle-hole types of excitations as in the Mott-insulator case. In Fig. 2(d), one observes a larger spread of the peaks as compared with the Mott-insulator case at the same Bragg angle. This is due to the larger value of the tunneling rate J . We remark that, choosing smaller values of the ratio U/J by ramping down the on-site interaction strength, as will be shown, the spectrum reduces to a single peak at all Bragg angles and approaches the limit of the single-particle spectrum, as it is recovered in Eq. (34) by setting $U = 0$.

We now compare the numerical results, obtained taking systematically into account the light-induced hopping term, to the results found when this term is neglected, corresponding to the treatment in [24]. In the Mott-insulator case, comparison between the numerical results with and without light-induced hopping effects shows that in the first case one finds interference between ordinary tunneling and light-induced hopping. This gives rise to an alternating enhancement and reduction

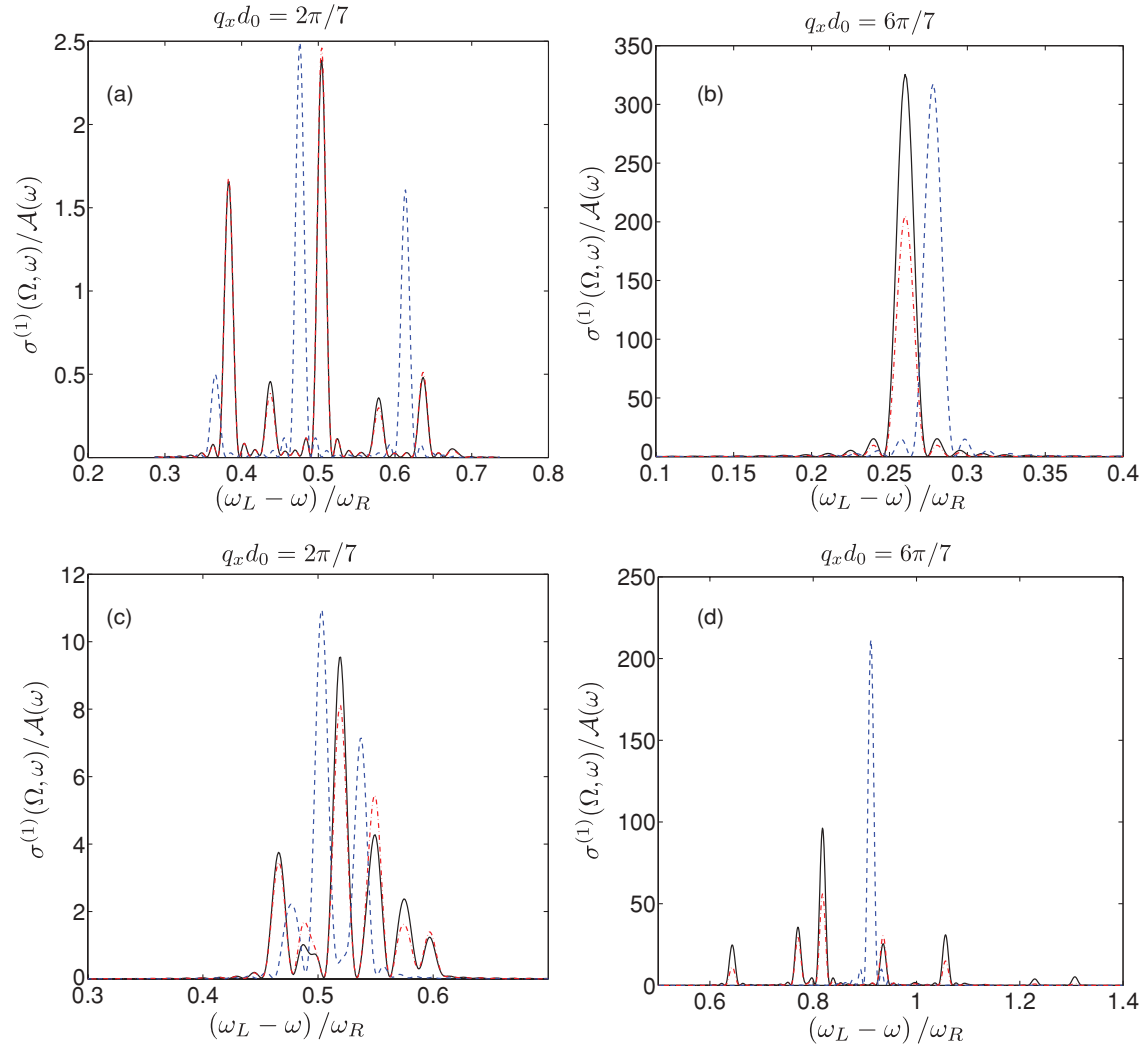


FIG. 2. (Color online) Stokes component of the differential scattering cross section [in units of $\mathcal{A}(\Omega)$] as a function of frequency (in units of the recoil frequency ω_R) for two different scattering angles, corresponding to $q_x d_0 = 2\pi/7$ (top row) and to $q_x d_0 = 6\pi/7$ (bottom row). The curves have been evaluated for a lattice of $M = 7$ site and $N = M = 7$ composed by ^{87}Rb atoms in the $|F = 2, m_F = 2\rangle$ hyperfine ground state. The black solid line corresponds to the numerical results, the blue dashed line to the analytical formulas (see text), and the red dashed-dotted line to the model of [24], where the light-induced hopping is neglected. Plots (a) and (c) are evaluated for $V_0 = 8.1 \hbar \omega_R$ ($U/J \approx 17$) which corresponds to the Mott-insulator state. Plots (b) and (d) are evaluated for $V_0 = 0.1 \hbar \omega_R$ ($U/J \approx 1$) which corresponds to the superfluid state. Other parameters are $d_0 = 413$ nm, $a_s = 105a_0$, with a_0 being the Bohr radius and $\omega_r = 10\omega_R$ corresponding to the experimental parameters in [22]. (For these parameters, the size of the radial wave packet is $\xi_r = 10a_s$.) The frequency resolution is set to $\Delta\omega = 300$ Hz, corresponding to an integration time $T = 3$ ms.

of the peak heights at different frequencies, which is absent in the model discarding light-induced hopping effects. In general, the light-hopping term contributes to determining the height of some peaks, giving substantial modifications of the spectrum which can be revealed experimentally. The effect is larger in the superfluid regime, where tunneling is enhanced, as one can see in Fig. 2(b). Here, the central peak at $q_x d_0 = 2\pi/7$ is 50% higher than in absence of this contribution.

Figures 3(a)–3(c) display the spectra of $\sigma^{(1)}$ as a function of the frequency and of the Bragg angle, in three different points of the phase diagram. We remark that the width and spacing of the Bragg peaks are determined by the finite size of the lattice. The plots in Figs. 2(a) and 2(b) are made in the same parameter regimes as in Figs. 2(a) and 2(c) and 2(b) and 2(d),

respectively, namely $U/J \approx 17$ and $U/J \approx 1$. Figure 3(c), instead, corresponds to the value $U/J \sim 0.1$. Here, one observes almost a single peak at each Bragg angle, as expected in the weakly interacting superfluid phase.

Figure 4 shows $\sigma^{(1)}$ as a function of the frequency and the depth of the potential, hence, sweeping from the Mott insulator to the superfluid regime at a given Bragg angle, corresponding to a large momentum transfer ($q_x d_0 = 6\pi/7$). Here, one observes that the spectrum varies from multiple peaks, deep in the Mott-insulator regime, to a single peak in the weakly interacting superfluid regime. The single peak appears around a value of U/J much smaller than the critical value $[U/J]_c$ for the Mott-to-superfluid transition (which, in the thermodynamic limit, is predicted for $[U/J]_c = 3.37$; see

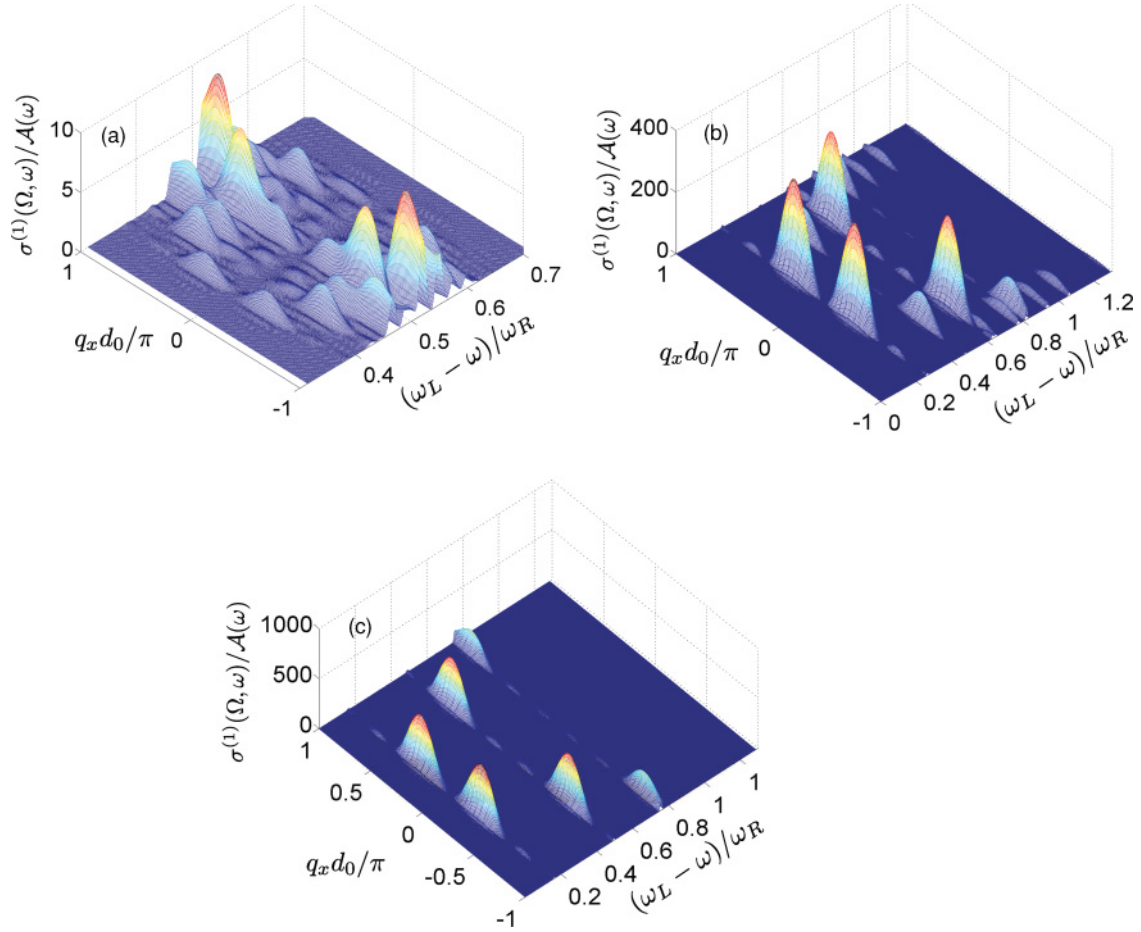


FIG. 3. (Color online) Stokes component of the differential scattering cross section [in units of $\mathcal{A}(\Omega)$] as a function of the frequency (in units of ω_R) and of the Bragg angle $\Theta = q_x d_0$ (in units of π). The plots have been evaluated numerically for (a) $V_0 = 8.1 \hbar \omega_R$ and $U/J \approx 17$, (b) $V_0 = 0.1 \hbar \omega_R$ and $U/J \approx 1$, and (c) $V_0 = 0.1 \hbar \omega_R$ and $U/J \approx 0.1$. The other parameters are as in Fig. 2.

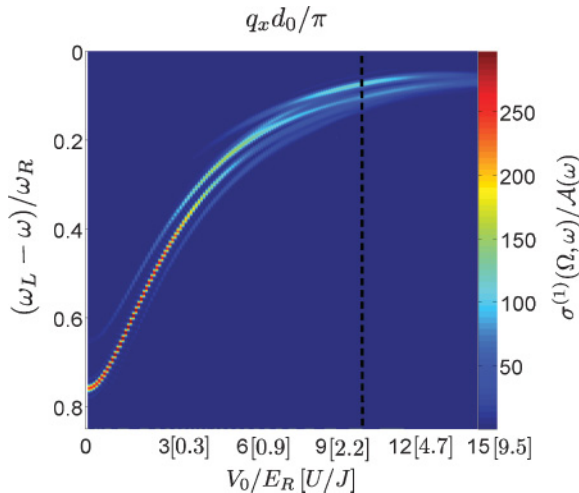


FIG. 4. (Color online) Contour plot of the Stokes component of the differential scattering cross section [in units of $\mathcal{A}(\Omega)$] as a function of the frequency (in units of ω_R) and of the lattice depth V_0 in units of ω_R for $q_x d_0 = 6\pi/7$ (the corresponding value of the ratio U/J is reported in the axis between the squared bracket). The black dashed line marks the critical value at which the phase transition occurs in the thermodynamic limit. The other parameters are given in Fig. 2.

Ref. [47]). The presence of multiple peaks also in the superfluid phase close to the phase transition is reminiscent of a strongly interacting superfluid phase. Such phase contains, beyond the gapless phononic modes, also gapped modes [48–52], which are predicted to be dominant at large quasimomentum. We expect that also in the thermodynamic limit the transition to a single peak in the scattered-light spectrum will occur at lower values of U/J than the Mott-insulator-to-superfluid phase transition and will be also dependent on the momentum transfer. The identification of the Mott-insulator-to-superfluid phase transition should rather rely on the existence of a gapless spectrum. Despite the very small size of the considered system, indications of a gapless spectrum are present in our results, as one can see comparing Fig. 3(a) with Figs. 3(b) and 3(c).

The intensity of the scattered light as a function of the Bragg angle is determined by the differential scattering cross section

$$\frac{d\sigma}{d\Omega} = \int d\omega \sigma(\Omega, \omega), \quad (55)$$

and is reported in Fig. 5 for the atoms in the Mott insulator [Fig. 5(a)] and in the superfluid state [Fig. 5(b)]. The solid line here corresponds to the numerical results, the dashed line to the analytical predictions, and the dashed-dotted line to the model where light-induced hopping has been discarded,

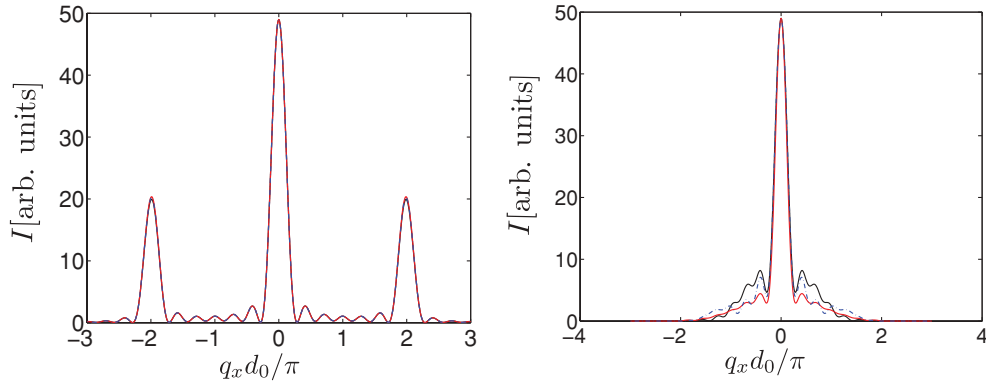


FIG. 5. (Color online) Intensity of the scattered light (in arbitrary units) as a function of the Bragg angle $\Theta = q_x d_0$ (in units of π). The parameters are the same as in Fig. 2 and (a) $V_0 = 8.1 E_R$ ($U/J \approx 17$) and (b) $V_0 = 0.1 E_R$ ($U/J \approx 1$). The black solid line corresponds to the numerical result, the blue dashed-dotted line to the analytical solution, and the red dashed line to the numerical result obtained discarding the light-induced hopping term as in [32] and [24].

which is similar to the case considered in Ref. [32]. In this latter work, in fact, corrections due to the tunneling J were neglected when evaluating light scattering by the atoms in the Mott-insulator state, while the calculation of light scattering from the superfluid state was made discarding the finite value of the on-site interaction as well as the finite width of the Wannier functions. In Fig. 5(a), we observe that in the Mott-insulator regime, the signal is dominated by the elastic component and corresponds to a classical diffraction grating. In the superfluid regime, on the other hand, one finds that the amplitude of the Bragg peak is modified, and a background signal appears which is due to light scattering by the condensate fraction. This signal is the signature of the superfluid phase, and it arises from the coherent effects of tunneling and light-induced hopping. We also notice that in the superfluid phase, only the first diffraction order is visible. This is due to the increased width of the atomic wave function, which yields a faster decaying Debye-Waller factor $J_0(\mathbf{q})$. We remark that higher diffraction orders would be visible if the superfluid regime was accessed by keeping the lattice depth constant, for instance by ramping down the on-site energy using a Feshbach resonance. The Bragg signal as a function of

the lattice depth is reported in Fig. 6, showing the appearance of the background signal as the superfluid regime is approached.

IV. CONCLUSIONS

We have discussed Bragg spectroscopy of ultracold bosonic atoms in an optical lattice, focusing on the signatures of the Mott insulator and superfluid quantum state in the scattered photons. A full quantum theory for the atoms and photons dynamics and interactions has been developed, allowing us to identify the various contributions to the detected signals. We have characterized the Bragg scattering signal for the parameters sweeping across the transition from the Mott insulator to the superfluid quantum state. In particular, the contribution of light-induced hopping, arising from atomic recoil due to photon scattering, has been put into evidence. This term has been neglected in previous theoretical treatments [24,32]. In this work, we have shown that its contribution can interfere with ordinary tunneling between sites, thereby significantly affecting the spectroscopic signal. Its effect is visible in the behavior of the height of the peaks in the spectrum as a function of the emission angle, and it has been singled out by comparing the spectrum evaluated when this effect is discarded. This effect can be revealed experimentally in large systems, according to the analytical theory we develop by extending the one derived in [24,42], and in small systems, as we observe by numerically evaluating the spectrum for a lattice of seven atoms. It is interesting to consider whether such properties can be used as resources for photonic interfaces based on strongly correlated atoms in optical lattices.

This analysis has been made in the linear regime, assuming a weak probe and far-off resonance both from the atoms and from the frequency of the lattice beam. Using instead Bragg beams at the same frequency as the optical lattice, wave-mixing effects are expected, as reported, for instance, in Refs. [4,5,53]. In addition, optical lattices have been discussed in the literature as a possible realization of photonic bandgap materials [15,54–60]. An interesting question is how such photonic properties are modified when the many-body quantum state of the atoms is relevant to the atom-photon interactions dynamics. When the light is close to resonance with the atoms, hence in

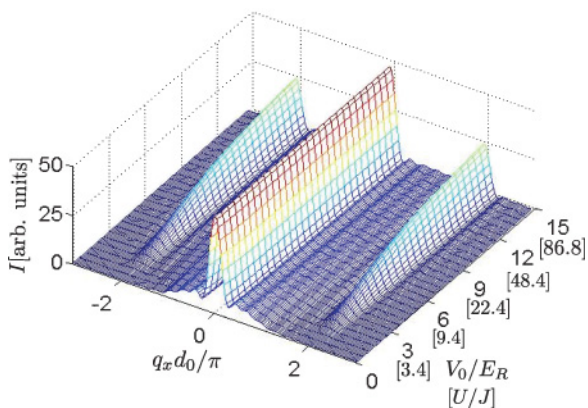


FIG. 6. (Color online) Intensity of the scattered light (in arbitrary units) as a function of the Bragg angle $\Theta = q_x d_0$ (in units of π) and of the lattice depth V_0 (in units of $\hbar \omega_R$) (the corresponding values of the ratio U/J are reported between squared brackets). The other parameters are reported in Fig. 2.

the dissipative regime, the state of the atoms is significantly heated up. On the other hand, interesting photon-photon correlations could be observed, due to interference in multiple scattering by the atoms (see, e.g., Ref. [61]).

We remark that, while monitoring the state of the gas by means of photons is attractive, Bragg spectroscopy modifies the atomic system, as the recoil imparted by the scattered photon significantly perturbs the state of the atomic gas. It would be desirable to identify schemes, such as the quantum nondemolition type of measurements [62,63], which can allow one to measure the relevant quantities in a noninvasive way. This may permit one to implement feedback mechanisms [36,64], which would allow one to prepare other nonclassical states of the atomic gas.

ACKNOWLEDGMENTS

The authors acknowledge Immanuel Bloch, Iacopo Carusotto, Igor Mekhov, Wolfgang Schleich, and Stefano Zippilli for stimulating discussions and helpful comments. This work was supported by the European Commission (EMALI, MRTN-CT-2006-035369; Integrated Project SCALA, Contract No. 015714), European Science Foundation (EUROQUAM “CMMC”), and Spanish Ministerio de Educación y Ciencia (Consolider-Ingenio 2010 QOIT, CSD2006-00019; QNLP, FIS2007-66944; Ramon-y-Cajal; Acción Integrada HU2007-0013). G.M. is supported by the DFG (German Research Council) with a Heisenberg professorship. C.M. thanks ICFO—The Institut for Photonic Sciences in Barcelona for hospitality during the period when this work was started.

-
- [1] N. W. Ashcroft and N. D. Mermin, *Solid State Physics* (Saunders College, Philadelphia, 1976).
- [2] W. M. Itano, J. J. Bollinger, J. N. Tan, B. Jelenkovic, X.-P. Huang, and D. J. Wineland, *Science* **279**, 686 (1998).
- [3] M. Weidemüller, A. Hemmerich, A. Görlitz, T. Esslinger, and T. W. Hänsch, *Phys. Rev. Lett.* **75**, 4583 (1995).
- [4] G. Birkl, M. Gatzke, I. H. Deutsch, S. L. Rolston, and W. D. Phillips, *Phys. Rev. Lett.* **75**, 2823 (1995).
- [5] G. Grynberg and C. Robilliard, *Phys. Rep.* **355**, 335 (2001).
- [6] L. Guidoni, C. Triché, P. Verkerk, and G. Grynberg, *Phys. Rev. Lett.* **79**, 3363 (1997).
- [7] S. Slama, C. von Cube, A. Ludewig, M. Kohler, C. Zimmermann, and Ph. W. Courteille, *Phys. Rev. A* **72**, 031402(R) (2005); S. Slama, C. von Cube, B. Deh, A. Ludewig, C. Zimmermann, and Ph. W. Courteille, *Phys. Rev. Lett.* **94**, 193901 (2005); S. Slama, C. von Cube, M. Kohler, C. Zimmermann, and Ph. W. Courteille, *Phys. Rev. A* **73**, 023424 (2006).
- [8] J. Stenger, S. Inouye, A. P. Chikkatur, D. M. Stamper-Kurn, D. E. Pritchard, and W. Ketterle, *Phys. Rev. Lett.* **82**, 4569 (1999); D. M. Stamper-Kurn, A. P. Chikkatur, A. Görlitz, S. Inouye, S. Gupta, D. E. Pritchard, and W. Ketterle, *ibid.* **83**, 2876 (1999).
- [9] R. Ozeri, N. Katz, J. Steinhauer, and N. Davidson, *Rev. Mod. Phys.* **77**, 187 (2005).
- [10] D. Clément, N. Fabbri, L. Fallani, C. Fort, and M. Inguscio, *Phys. Rev. Lett.* **102**, 155301 (2009).
- [11] S. Pirandola, S. Mancini, D. Vitali, and P. Tombesi, *Phys. Rev. A* **68**, 062317 (2003).
- [12] J. I. Cirac, R. Blatt, A. S. Parkins, and P. Zoller, *Phys. Rev. A* **48**, 2169 (1993); Ch. Raab, J. Eschner, J. Bolle, H. Oberst, F. Schmidt-Kaler, and R. Blatt, *Phys. Rev. Lett.* **85**, 538 (2000).
- [13] S. Mancini, D. Vitali, and P. Tombesi, *Phys. Rev. Lett.* **90**, 137901 (2003).
- [14] G. Morigi, J. Eschner, S. Mancini, and D. Vitali, *Phys. Rev. Lett.* **96**, 023601 (2006).
- [15] I. H. Deutsch, R. J. C. Spreeuw, S. L. Rolston, and W. D. Phillips, *Phys. Rev. A* **52**, 1394 (1995).
- [16] M. Weidemüller, A. Görlitz, T. W. Hänsch, and A. Hemmerich, *Phys. Rev. A* **58**, 4647 (1998).
- [17] B. Nagorny, Th. Elsässer, and A. Hemmerich, *Phys. Rev. Lett.* **91**, 153003 (2003); D. Kruse, C. von Cube, C. Zimmermann, and Ph. W. Courteille, *ibid.* **91**, 183601 (2003).
- [18] I. Bloch, J. Dalibard, and W. Zwerger, *Rev. Mod. Phys.* **80**, 885 (2008).
- [19] D. Jaksch, C. Bruder, J. I. Cirac, C. W. Gardiner, and P. Zoller, *Phys. Rev. Lett.* **81**, 3108 (1998).
- [20] M. Lewenstein, A. Sanpera, V. Ahufinger, B. Damski, A. Sen De, and U. Sen, *Adv. Phys.* **56**, 243 (2007).
- [21] M. Greiner, O. Mandel, T. Esslinger, T. W. Hänsch, and I. Bloch, *Nature* **415**, 39 (2002).
- [22] T. Stöferle, H. Moritz, C. Schori, M. Köhl, and T. Esslinger, *Phys. Rev. Lett.* **92**, 130403 (2004).
- [23] M. Krämer, C. Tozzo, and F. Dalfovo, *Phys. Rev. A* **71**, 061602(R) (2005).
- [24] A. M. Rey, P. B. Blakie, G. Pupillo, C. J. Williams, and C. W. Clark, *Phys. Rev. A* **72**, 023407 (2005).
- [25] A. Brunello, F. Dalfovo, L. Pitaevskii, S. Stringari, and F. Zambelli, *Phys. Rev. A* **64**, 063614 (2001).
- [26] C. Menotti, M. Krämer, L. Pitaevskii, and S. Stringari, *Phys. Rev. A* **67**, 053609 (2003).
- [27] H. W. Chan, A. T. Black, and V. Vuletic, *Phys. Rev. Lett.* **90**, 063003 (2003); A. T. Black, H. W. Chan, and V. Vuletic, *ibid.* **91**, 203001 (2003).
- [28] F. Brennecke, T. Donner, S. Ritter, T. Bourdel, M. Köhl, and T. Esslinger, *Nature (London)* **450**, 268 (2007); F. Brennecke, S. Ritter, T. Donner, and T. Esslinger, *Science* **322**, 235 (2008).
- [29] Y. Colombe, T. Steinmetz, G. Dubois, F. Linke, D. Hunger, and J. Reichel, *Nature (London)* **450**, 272 (2007).
- [30] S. Gupta, K. L. Moore, K. W. Murch, and D. M. Stamper-Kurn, *Phys. Rev. Lett.* **99**, 213601 (2007); K. W. Murch, K. L. Moore, S. Gupta, and D. M. Stamper-Kurn, *Nature Phys.* **4**, 561 (2008).
- [31] P. Cañizares, T. Görler, J. P. Paz, G. Morigi, and W. P. Schleich, *Laser Phys.* **17**, 903 (2007).
- [32] I. B. Mekhov, C. Maschler, and H. Ritsch, *Phys. Rev. Lett.* **98**, 100402 (2007); *Phys. Rev. A* **76**, 053618 (2007).
- [33] W. Chen, D. Meiser, and P. Meystre, *Phys. Rev. A* **75**, 023812 (2007).
- [34] I. B. Mekhov, C. Maschler, and H. Ritsch, *Nature Phys.* **3**, 319 (2007).

- [35] J. Larson, B. Damski, G. Morigi, and M. Lewenstein, *Phys. Rev. Lett.* **100**, 050401 (2008).
- [36] I. B. Mekhov and H. Ritsch, *Phys. Rev. Lett.* **102**, 020403 (2009).
- [37] J. Ruostekoski, C. J. Foot, and A. B. Deb, *Phys. Rev. Lett.* **103**, 170404 (2009).
- [38] J. Javanainen and J. Ruostekoski, *Phys. Rev. Lett.* **91**, 150404 (2003); J. Ruostekoski, J. Javanainen, and G. V. Dunne, *Phys. Rev. A* **77**, 013603 (2008).
- [39] M. Lewenstein, L. You, J. Cooper, and K. Burnett, *Phys. Rev. A* **50**, 2207 (1994).
- [40] C. Cohen-Tannoudji, J. Dupont-Roc, and G. Grynberg, *Atom-Photon Interactions* (Wiley, New York, 2004).
- [41] M. Saba, T. A. Pasquini, C. Sanner, Y. Shin, W. Ketterle, and D. E. Pritchard, *Science* **307**, 1945 (2005).
- [42] A. M. Rey, Ph.D. thesis, University of Maryland, 2004 (<http://jilawww.colorado.edu/~arey/papers/thesis.pdf>).
- [43] L. Pitaevski and S. Stringari, *Bose-Einstein Condensation* (Oxford Science, Oxford, UK, 2003).
- [44] Equation (44) is reported with the density of states at the value of the laser frequency ω_L . This approximation is justified, as the range of frequencies of the final states is of the order of the recoil frequency (from few to tens KHz), while the laser frequency is in the optical regime. The same approximation will be applied to the vacuum coupling strengths C_λ , Eq. (6), entering the interaction Hamiltonian H'_{int} , Eq. (8).
- [45] While in general the use of the Gaussian ansatz in place of Wannier functions should be handled with care, as Wannier functions decay exponentially at infinity [see, e.g., W. Kohn, *Phys. Rev.* **115**, 809 (1959)], the precise form of the ansatz is not important for the purpose of this estimate.
- [46] The linewidth of the excitations is essentially determined by the spontaneous decay rate of the excited state. In this treatment, we are assuming $\gamma'T \ll 1$, where γ' is the rate of incoherent scattering and is of the order $\gamma' \sim \gamma C_L \alpha^2 / \Delta^2$.
- [47] T. D. Kühner, S. R. White, and H. Monien, *Phys. Rev. B* **61**, 12474 (2000).
- [48] K. Sengupta and N. Dupuis, *Phys. Rev. A* **71**, 033629 (2005).
- [49] S. Konabe, T. Nikuni, and M. Nakamura, *Phys. Rev. A* **73**, 033621 (2006).
- [50] Y. Ohashi, M. Kitaura, and H. Matsumoto, *Phys. Rev. A* **73**, 033617 (2006).
- [51] S. D. Huber, E. Altman, H. P. Büchler, and G. Blatter, *Phys. Rev. B* **75**, 085106 (2007).
- [52] C. Menotti and N. Trivedi, *Phys. Rev. B* **77**, 235120 (2008).
- [53] S. Guibal, C. Mennerat-Robilliard, D. Larousserie, C. Triche, J. Y. Courtois, and G. Grynberg, *Phys. Rev. Lett.* **78**, 4709 (1997).
- [54] D. V. van Coevorden, R. Sprik, A. Tip, and A. Lagendijk, *Phys. Rev. Lett.* **77**, 2412 (1996).
- [55] P. Lambropoulos, G. M. Nikolopoulos, T. R. Nielsen, and S. Bay, *Rep. Prog. Phys.* **63**, 455 (2000).
- [56] M. Artoni, G. La Rocca, and F. Bassani, *Phys. Rev. E* **72**, 046604 (2005).
- [57] Y. D. Chong, D. E. Pritchard, and M. Soljacic, *Phys. Rev. B* **75**, 235124 (2007).
- [58] I. Carusotto, M. Antezza, F. Bariani, S. De Liberato, and C. Ciuti, *Phys. Rev. A* **77**, 063621 (2008); F. Bariani and I. Carusotto, *J. Eur. Opt. Soc.* **3**, 08005 (2008).
- [59] S. Rist, P. Vignolo, and G. Morigi, *Phys. Rev. A* **79**, 053822 (2009).
- [60] M. Antezza and Y. Castin, *Phys. Rev. A* **80**, 013816 (2009).
- [61] S. Rist, J. Eschner, M. Hennrich, and G. Morigi, *Phys. Rev. A* **78**, 013808 (2008).
- [62] K. Ekert, O. Romero Isart, M. Rodriguez, M. Lewenstein, E. Polzik, and A. Sanpera, *Nature Phys.* **4**, 50 (2008).
- [63] V. B. Braginsky and F. Y. Khalili, in *Quantum Measurement*, edited by K. S. Thorne (Cambridge University, New York, 1995).
- [64] P. Bushev, D. Rotter, A. Wilson, F. Dubin, C. Becher, J. Eschner, R. Blatt, V. Steixner, P. Rabl, and P. Zoller, *Phys. Rev. Lett.* **96**, 043003 (2006).